$$AlH_3 + BeCl_2 \rightarrow H_2AlCl + HBeCl \quad (5)$$

At an AlH_3:$BeCl_2$ ratio of 2:1, the infrared spectrum showed bands at 1850 (sh), 1788, 970, 905, 772, and 725 cm^{-1}. These data correspond to a mixture of AlH_3 and H_2AlCl. The bands at 970 and 905 cm^{-1} are again attributed to HBeCl. A small amount of solid precipitated from the reaction mixture. The solid was found to be BeH_2 and represented 6% of the total beryllium added. At AlH_3:$BeCl_2$ ratios of 4:1 and 8:1 larger amounts of solid were isolated. This solid proved to be BeH_2 in yields of 34.8 and 56%, respectively. Alane was also found to reduce HBeCl in ether to BeH_2 in 63% yield (based on HBeCl) at an AlH_3:HBeCl ratio of 2:1 (eq 6).

$$2AlH_3 + HBeCl \rightleftharpoons BeH_2\downarrow + H_2AlCl + AlH_3 \quad (6)$$

The compound HBeCl was prepared independently by the redistribution of BeH_2 and $BeCl_2$ in ether (eq 7). The

$$BeH_2 + BeCl_2 \rightarrow 2HBeCl \quad (7)$$

infrared spectrum of HBeCl in ether showed bands at 1330, 1050, 970, 908, 840 (sh), 790, and 700 cm^{-1}. The infrared spectrum of DBeCl showed that the band at 1330 cm^{-1} shifted to 985 cm^{-1} and the band at 970 cm^{-1} in HBeCl disappeared in DBeCl. This gives a ν_H:ν_D ratio of 1.35. Molecular weight determination of HBeCl in ether indicates that the compound is associated with an *i* value of 2.17 at 0.1-0.3 *m*.

Coates and Roberts[9] isolated the complex Be_2H_4·TMED which has a sharp doublet in the infrared spectrum at 1787 and 1807 cm^{-1}. They attribute these bands to terminal Be-H stretching vibrations. We find no bands in this region for HBeCl. Bell and Coates[10] have reported the compounds $[CH_3BeH{\cdot}N(CH_3)_3]_2$ and $[C_2H_5BeH{\cdot}N(CH_3)_3]_2$ which are dimers in benzene. These compounds exhibit strong absorption at 1333-1344 cm^{-1} (in cyclohexane) which is attributed to the Be-H-Be bridge. In the deuterated compounds, the 1344-cm^{-1} band of $[CH_3BeH{\cdot}N(CH_3)_3]_2$ shifted to 1020 cm^{-1}. We therefore conclude that HBeCl is associated through Be-H-Be bridge bonds, *i.e.*

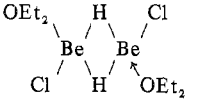

Acknowledgment. We acknowledge with gratitude support of this work by the Office of Naval Research.

Registry No. $BeCl_2$, 7787-47-5; $LiAlH_4$, 16853-85-3; AlH_3, 7784-21-6; HBeCl, 42016-55-7; $[HBeCl(OEt_2)]_2$, 42744-98-9.

(9) G. E. Coates and P. D. Roberts, *J. Chem. Soc. A*, 1008 (1969).
(10) N. A. Bell and G. E. Coates, *J. Chem. Soc.*, 692 (1965).

Contribution from the National Institute of Dental Research, National Institutes of Health, Bethesda, Maryland 20014

Infrared Studies of Apatites. I. Vibrational Assignments for Calcium, Strontium, and Barium Hydroxyapatites Utilizing Isotopic Substitution

B. O. FOWLER

Received July 11, 1973

The infrared spectra of powdered calcium hydroxyapatite isotopically substituted with D, ^{18}O, ^{44}Ca, and ^{48}Ca and infrared spectra of powdered strontium and barium hydroxyapatites and their deuterated analogs are reported at 48 and −185° in the 4000-200-cm^{-1} region. Band assignments, based on isotopic frequency shifts, band intensity, band temperature dependency, and comparisons between corresponding bands of these structurally related apatites are presented for the above and other apatites.

Introduction

The major crystalline calcium phosphate in teeth and bones is well known to have an apatite-like structure; however, many compositional and structural details of both the *in vitro* and *in vivo* apatites have not been clearly resolved. Consequently, numerous chemical and physical studies of the biological apatites, synthetic apatites, geological apatites, and related calcium phosphates have been carried out to acquire further knowledge to define better the chemical and structural details of the apatites. One effectual physical method for studying both compositional and structural details of the apatites is infrared spectroscopy. The initial requirements to utilize effectively the infrared data for determining compositional and structural details are the complete assignment and characterization of the vibrational spectra of the pure apatite end members of controlled chemical and physical properties.

Spectral assignment and characterization should be made on oriented single crystals using polarized radiation and also on powdered samples, progressively reduced in particle size to a few unit cells. Single-crystal studies provide data necessary for more complete spectral assignments including spatial vibrational transition moments and bond directions whereas the powder data represent an average spectrum reflecting all orientations of the crystallites. The small crystal size of most apatites of controlled chemical composition generally precludes oriented single-crystal analysis, and, therefore, powder data are usually obtained. The small crystal size of many biological and other apatites render powder data appropriate along with spectral characterization of extremely small apatite crystals (a few unit cells). Extremely small pure apatite crystals may show spectral alteration due to both surface and size effects independent of vibrational perturbations expected to arise from additional sources in extremely small impure apatites. The powdered apatites examined in this study were prepared under controlled conditions in order to minimize the occurrence of absorption bands and/or perturbation in vibrational frequencies and intensities arising from, *e.g.*, nonstoichiometry, substitution of other ions, impurities, size, surface effects, and poor crystal perfection.

The following powdered synthetic apatites were studied spectrally at 48 and −185°: calcium hydroxyapatite, $Ca_{10}(PO_4)_6(OH)_2$, Ca(OH)A; strontium hydroxyapatite, $Sr_{10}(PO_4)_6(OH)_2$, Sr(OH)A; barium hydroxyapatite, $Ba_{10}(PO_4)_6(OH)_2$, Ba(OH)A. Spectra of these apatites are assigned and/or characterized in the 4000–200-cm^{-1} region, and band assignments for other apatites are also given. These assignments are based on isotopic frequency shifts (D, ^{18}O, ^{44}Ca, ^{48}Ca), band intensity, band temperature dependency, and comparisons between corresponding bands of these structurally related apatites. The spectra are discussed in terms of bands predicted according to site and factor group symmetry analyses.

Experimental Section

Apatite Samples. The apatites were prepared according to the procedures given in the following paper.[1]

Infrared Absorption Measurements. Spectra from 4000 to 200 cm^{-1} of the powdered apatite samples less than 5 μ in particle size suspended in KBr or CsI pellets or mulled in Nujol were recorded using a Perkin-Elmer Model 621 spectrophotometer purged with dry air. Spectra of the Ca (except the ^{18}O-enriched sample), Sr, and Ba apatites in Figures 1 and 4 from 4000 to 400 cm^{-1} were recorded using circular 13-mm diameter, 400-mg KBr pellets containing equivalent molar concentrations, 0.60, 0.89, and 1.19 mg of the apatites, respectively, pressed in an evacuated die under a total force of 10 tons for 2 min. The Ca(^{18}OH)A spectrum in Figure 1 was recorded from 4000 to 200 cm^{-1} using a CsI pellet. Spectra from 400 to 200 cm^{-1} in Figures 1 and 4 and from 1150 to 200 cm^{-1} at 48° in Figures 2 and 5 were recorded using 600-mg CsI pellets and the same apatite concentrations as above. Nearly transparent 13-mm diameter CsI pellets were obtained by pressing in an evacuated die under a total force of 10 tons for 30 sec and then pressing consecutively ten times at 4 tons for 5-sec intervals.

Spectra in Figure 6 were obtained from the apatites mulled in Nujol; the apatite sample concentrations for these spectra correspond to about 60 times those used for the spectra in Figures 1 and 4.

The spectra were recorded at 48 and −185°. The 48° temperature was not controlled but was the nearly constant temperature of the sample pellet in the infrared beam of the spectrophotometer in ambient surroundings.

Spectra of the apatites at −185° were obtained using a Beckman VLT-2 low-temperature cell equipped with CsI windows and cooled with liquid nitrogen. A cold trap, cooled with liquid nitrogen, was placed between the low-temperature cell and the vacuum pump to minimize spectral bands resulting from condensation of vapors on the cooled sample-containing pellet. One-gram KBr or 2-g CsI pellets 25 mm in diameter containing 2.00, 2.96, and 3.96 mg of the Ca, Sr, and Ba apatites, respectively, were placed in the standard VLT-2 solids holder having a 10 × 24 mm opening which allowed sufficient energy to pass for good instrument response. All the spectra at −185° from 1150 to 200 cm^{-1} were recorded using CsI pellets. The 25-mm diameter pellets were pressed at about the same pressure as the 13-mm diameter pellets which required a total force of 40 tons. Blank pellets were placed in the reference beam and interference fringes arising from the pellets were minimized by roughening the pellet surfaces with a cotton towel.

The absolute wave number (referred to hereafter as frequency) accuracy was 1–2 cm^{-1}, and precision in measuring shifts in sharp bands was usually less than 1 cm^{-1}. Broad bands and bands occurring as shoulders with an uncertainty of several reciprocal centimeters in maxima are preceded by the symbol ~ in the tables.

Results

The infrared spectra of Ca-, Sr-, and Ba(OH)A, their deuterated analogs, and ^{18}O-enriched Ca apatite from 4000 to 200 cm^{-1} at 48° are shown in Figures 1 and 4; the band frequencies and assignments are given in Tables IV and VIII. Spectra of the deuterated Ca, Sr, and Ba apatites indicate about 95, 90, and 70% OD substitution, respectively, as estimated from reduction in OH band intensities. The Ca(^{18}OH)A is estimated to contain about 80% of the total oxygen as oxygen-18.

Expanded abscissa scale spectra from 1150 to 200 cm^{-1} at 48 and −185° are shown in Figures 2 and 5 and at −185° in Figure 3. No additional apatite bands or significant spectral differences were observed in the 4000–1150-cm^{-1} region at −185°, except for slight band shifts to higher frequencies, and this spectral region at −185° is not shown.

The frequencies, approximate frequency shifts, and new bands observed at −185° for the apatites are given in Tables IV and VIII. Except for the Ca-, Sr-, and Ba(OH)A bands at 630, 535, and 430 cm^{-1}, respectively, which shift to lower frequencies at −185°, the other bands shift (except for one band in the 560-cm^{-1} region), the lower frequency bands shifting more, to higher frequencies. The increases in band intensity, sharpness, and resolution at −185° are evident in the spectra; these changes are more marked in the 500–200-cm^{-1} region and especially in the spectra of the Ba(OH) and -(OD) apatites in Figure 5.

Comparisons of the calculated and observed frequency shifts and/or frequency ratios on isotopic substitution (^{18}O and D) for specific vibrational modes are given in Tables IV and VI, and the frequency shifts on isotopic Ca substitution are given in Table V.

Spectra of Ca-, Sr-, and Ba(OH)A from 2300 to 1800 cm^{-1} at 48° are shown in Figure 6, and the frequencies and assignments are given in Table IX.

Although the complete infrared spectrum of calcium fluorapatite (CaFA) is not discussed in this paper, the CaFA vibrational selection rules are given because of structural similarities between Ca(OH)A and CaFA. The vibrational selection rules and a summary are given in Tables I–III. The apatite crystal structure data were obtained from Kay, *et al.*,[2] and from the "International Tables for X-Ray Crystallography," Vol. I (International Union of Crystallography, 1952). The correlation method[3] was used to determine the factor group modes.

Apatite Structure and Vibrational Selection Rules

The apatites Ca(OH)A and CaFA have hexagonal structures and belong to the space groups $P6_3$ and $P6_3/m$, respectively. The apatite unit cell contains one $M_{10}(PO_4)_6X_2$ unit; the site symmetries of the ions are given in Tables I and II. The lower symmetry of the Ca(OH)A lattice results from both the position and the heteronuclearity of the OH ion. The F ions in CaFA are located along the sixfold screw axis on the mirror planes passing through the Ca_{II} triangles. In Ca(OH)A, the OH ions, with internuclear axes coincident with the sixfold screw axis, are displaced about 0.3 Å either above or below the mirror plane passing through the Ca_{II} triangles. The OH ion displacement (and heteronuclearity) removes the mirror plane and lowers the unit cell symmetry to $P6_3$ although the predominant lattice symmetry with respect to the Ca and PO_4 ions is still $P6_3/m$. This slight structural difference markedly changes the factor group selection rules for Ca(OH)A as compared to those of CaFA.

The 44 atoms of the Ca(OH)A unit cell give rise to 132 vibrational modes which are distributed as follows: 54 internal PO_4 modes, 2 internal OH modes, 18 libratory PO_4 lattice modes, 4 libratory OH lattice modes, and 54 translatory lattice modes resulting from translations of the 18 ions in the unit cell. The internal and lattice modes are further subdivided into groups which are dictated by the internal symmetry of each ion and the symmetry of the unit

(1) B. O. Fowler, *Inorg. Chem.*, 13, 207 (1974).

(2) M. I. Kay, R. A. Young, and A. S. Posner, *Nature (London)*, 204, 1050 (1964).

(3) W. G. Fateley, N. T. McDevitt, and F. F. Bentley, *Appl. Spectrosc.*, 25, 155 (1971).

Table I. Correlation Diagram and Spectral Activity for Internal and External Modes[a] of $Ca_{10}(PO_4)_6(OH)_2$ (Space Group $P6_3$)

Ions	Modes: External	Modes: Internal	Point group symmetry	Site group symmetry	Factor group symmetry, C_6
6 PO_4	---	ν_1	T_d: $A_1(R)$	C_1: A(I, R)	A(I, R) + B(0) + E_1(I, R) + E_2(R)
	---	ν_2	E(R)	2 A(I, R)	2 A(I, R) + 2 B(0) + 2 E_1(I, R) + 2 E_2(R)
	Trans	ν_3, ν_4	F_2(I, R)	3 A(I, R)	3 A(I, R) + 3 B(0) + 3 E_1(I, R) + 3 E_2(R)
	Lib		F_1(0)		
2 OH	Trans	Str	$C_{\infty v}$: Σ^+(I, R)	C_3: A(I, R)	A(I, R) + B(0)
	Trans, lib		Π(I, R)	E(I, R)	E_1(I, R) + E_2(R)
6 Ca_{II}	Trans			C_1: 3 A(I, R)	3 A(I, R) + 3 B(0) + 3 E_1(I, R) + 3 E_2(R)
4 Ca_I	Trans			C_3: A(I, R)	2 A(I, R) + 2 B(0)
				E(I, R)	2 E_1(I, R) + 2 E_2(R)

[a] I = infrared active; R = Raman active; 0 = inactive in both infrared and Raman spectra. One each of the 9 A and 9 E_1 factor group translatory external modes are acoustic modes. The two nonequivalent calcium positions are designated I and II. Total vibrations: $3n$ = 3(44) = 132 (site group check 132; factor group check 132).

Table II. Correlation Diagram and Spectral Activity for Internal and External Modes[a] of $Ca_{10}(PO_4)_6F_2$ (Space Group $P6_3/m$)

Ions	Modes: External	Modes: Internal	Point group symmetry	Site group symmetry	Factor group symmetry, C_{6h}
6 PO_4	---	ν_1	T_d: $A_1(R)$	C_s: A'(I, R)	$A_g(R) + E_{2g}(R) + B_u(0) + E_{1u}(I)$
	---	ν_2	E(R)	2 A'(I, R)	$2 A_g(R) + 2 E_{2g}(R) + 2 B_u(0) + 2 E_{1u}(I)$
	Trans	ν_3, ν_4	F_2(I, R)	A''(I, R)	$B_g(0) + E_{1g}(R) + E_{2u}(0) + A_u(I)$
	Lib		F_1(0)	2 A''(I, R)	$2 B_g(0) + 2 E_{1g}(R) + 2 E_{2u}(0) + 2 A_u(I)$
2 F	Trans			C_{3h}: E'(I, R)	$E_{2g}(R) + E_{1u}(I)$
				A''(I)	$B_g(0) + A_u(I)$
6 Ca_{II}	Trans			C_s: 2 A'(I, R)	$2 A_g(R) + 2 E_{2g}(R) + 2 B_u(0) + 2 E_{1u}(I)$
				A''(I, R)	$B_g(0) + E_{1g}(R) + E_{2u}(0) + A_u(I)$
4 Ca_I	Trans			C_3: E(I, R)	$E_{1g}(R) + E_{2g}(R) + E_{1u}(I) + E_{2u}(0)$
				A(I, R)	$A_g(R) + B_g(0) + A_u(I) + B_u(0)$

[a] I = infrared active; R = Raman active; 0 = inactive in both infrared and Raman spectra. One each of the 6 E_{1u} and 4 A_u factor group translatory external modes are acoustic modes. The two nonequivalent calcium positions are designated I and II. Total vibrations: $3n$ = 3(42) = 126 (site group check 126; factor group check 126).

cell. Correlation diagrams relating the modes and spectral activity of the ions in Ca(OH)A and CaFA under point group symmetry to the lattice site group symmetry and the latter to factor group or unit cell group symmetry are given in Tables I and II along with a summary in Table III. Site group analysis of Ca(OH)A predicts a total of 24 infrared-active modes whereas factor group analysis, which allows for coupling between modes of the ions in the unit cell,[4] predicts 42 infrared-active modes comprised of 18 internal PO_4 modes, 1 internal OH stretching mode, and 23 lattice modes distributed among 6 libratory PO_4 lattice modes, 1 libratory OH lattice mode, and 16 translatory lattice modes (Table III). Factor group analysis predicts a total of 20 infrared active modes for CaFA as compared to 40 for Ca(OH)A (excluding OH stretching and libration); this large difference in selection rules arises from the slight displacement and heteronuclearity of the OH ion.

Band Assignments and Discussion

Calcium Hydroxyapatite. Classifications of the internal PO_4 modes in Ca(OH)A according to site and factor group symmetry analyses are given in Tables I and III. The previously given assignments for the internal ν_3, ν_1, and ν_4 PO_4 modes[5-7] and reassignments[8-10] for the internal ν_2 PO_4 mode are as follows: the band at 1092 cm^{-1} and the doublet at about 1040 cm^{-1} were assigned to components of the triply degenerate ν_3 antisymmetric PO stretching mode; the 962-cm^{-1} band was assigned to ν_1, the nondegenerate PO symmetric stretching mode; the bands at 601, 575, and 561 cm^{-1} were assigned to components of the triply degenerate ν_4 OPO bending mode; and the bands at 474 and 465 cm^{-1} were assigned to components of the doubly degenerate ν_2 OPO bending mode.

Three major Ca(OH)A bands occur in the 400-200 cm^{-1} region at 343, about 282, and 228 cm^{-1}. The band at 343

(4) H. Winston and R. S. Halford, *J. Chem. Phys.*, 17, 607 (1949).

(5) B. O. Fowler, E. C. Moreno, and W. E. Brown, *Arch. Oral Biol.*, 11, 477 (1966).

(6) C. B. Baddiel and E. E. Berry, *Spectrochim. Acta*, 22, 1407 (1966).

(7) J. M. Stutman, J. D. Termine, and A. S. Posner, *Trans. N. Y. Acad. Sci.*, 27, 669 (1965).

(8) B. O. Fowler in "International Symposium on Structural Properties of Hydroxyapatite and Related Compounds, Gaithersburg, Md., Sept 12-14, 1968," Gordon and Breach, N. Y., New York, in press.

(9) S. R. Levitt, K. C. Blakeslee, and R. A. Condrate, Sr., *Mem. Soc. Roy. Sci. Liege*, 20, 121 (1970).

(10) K. C. Blakeslee and R. A. Condrate, Sr., *J. Amer. Ceram. Soc.*, 54, 559 (1971).

Table III. Predicted Number and Coincidence of Spectrally Active Internal and Lattice Modes[a,b] for $Ca_{10}(PO_4)_6F_2$ and $Ca_{10}(PO_4)_6(OH)_2$ According to Site Group and Factor Group Analyses

		Internal modes												Lattice modes							
		6 PO_4										2 OH		Libratory				Translatory			
		ν_1		ν_2		ν_3		ν_4		Total		Str		6 PO_4		2 OH		10 Ca, 6 PO_4, 2 X[f]		Total	
		c	nc	c	nc	c	nc	c	nc	c	nc	c	nc	c	nc	c	nc	c	nc	c	nc
										$Ca_{10}(PO_4)_6F_2$											
Site group[c]	I	1		2		3		3		9		...		3		...		9	1	12	1
	R	1		2		3		3		9		...		3		...		9		12	
C_{6h} factor group	I		1		2		3		3		9	...			3	...			10[e]		13[e]
	R		2		3		5		5		15	...			4	...			14		18
										$Ca_{10}(PO_4)_6(OH)_2$											
Site group[d]	I	1		2		3		3		9		1		3		1		10		14	
	R	1		2		3		3		9		1		3		1		10		14	
C_6 factor group	I	2		4		6		6		18		1		6		1		18[e]		25[e]	
	R	2	1	4	2	6	3	6	3	18	9	1		6	3	1	1	18[e]	9	25[e]	13

[a] I = infrared active; R = Raman active. [b] c = coincident; nc = noncoincident. [c] See Table II. [d] See Table I. [e] Two of these are acoustic modes. [f] X = OH or F.

cm^{-1} has a shoulder at about 355 cm^{-1} and the band centered at 282 cm^{-1} is a poorly resolved doublet with maxima at about 290 and 275 cm^{-1}; at −185° the doublet is well resolved and additional fine structure is evident in the 325-200-cm^{-1} region.

The OH stretching mode,[11] 3572 cm^{-1}, and the OH librational mode,[5] 630 cm^{-1}, have been assigned with certainty on the basis of deuteration shifts.

In the next three sections, isotopic substitution (^{18}O, D, ^{44}Ca, ^{48}Ca), relative band intensity comparisons, and band temperature dependency are used to examine the previous Ca(OH)A band assignments, with emphasis on the bands in the 500-200-cm^{-1} region.

Phosphate Modes in Oxygen-18-Enriched Apatite. The infrared spectra of Ca(OH)A containing approximately 80% of the total oxygen as ^{18}O (Figures 1 and 2; Table IV) showed distinct band shifts. All the previously assigned phosphate bands shifted to lower frequencies. The rigorous isotopic frequency shift relations according to the Teller-Redlich product rule restrict the frequency shift calculations to $P(^{16}O)_4$, $P(^{18}O)_4$ vibrations involving the same symmetry types. Under C_1 selection rules the nine internal phosphate vibrational modes are of symmetry type A which permits only one equation which is of little value in checking the frequency assignments. For tetrahedral symmetries of the $P(^{16}O)_4$, $P(^{18}O)_4$ isotopic pair according to Rosenthal[12] and the Teller-Redlich product rule, the following frequency relations exist[13]

$$\omega^i_1/\omega_1 = \omega^i_2/\omega_2 = (m_y/m^i_y)^{1/2} = 0.943$$

$$\omega^i_3\omega^i_4/\omega_3\omega_4 = m_y/m^i_y[(m_x m^i_x + 4m_x m^i_y)/(m_x m^i_x + 4m_y m^i_x)]^{1/2} = 0.926$$

where $\omega \cong \nu$, m_x and m_y are the masses of normal phosphorus and oxygen, respectively, and i denotes the isotopic mass or frequency. For small isotopic mass differences (*i.e.*, ^{18}O substituting for ^{16}O), the ν_1 and ν_2 frequency shifts for the progressively substituted groups $P(^{16}O)_3(^{18}O)$, $P(^{16}O)_2(^{18}O)_2$, and $P(^{16}O)(^{18}O)_3$ are respectively approximately one-fourth, half, and three-fourths that of the calculated shift for the fully substituted $P(^{18}O)_4$ group;[13] these calculated shifts are listed in Table IV.

In the ν_1 region of ^{18}O-substituted Ca(OH)A three bands were observed at 932, 919, and 908 cm^{-1} with relative intensities of approximately 1, 3, and 2, respectively. Spectra of the Ca(OH)A samples containing less ^{18}O had an additional band at 945 cm^{-1} corresponding to the $P(^{16}O)_3(^{18}O)$ group. The ν_1 frequency shifts, according to the tetrahedral model and the relative band intensities, indicated that this ^{18}O-enriched apatite contained about one $P(^{16}O)_2(^{18}O)_2$ group and three $P(^{16}O)(^{18}O)_3$ groups for every two $P(^{18}O)_4$ groups. The observed $P(^{18}O)_4$ band at 908 cm^{-1} (Table IV) is at nearly the exact frequency predicted for the ν_1 isotopic frequency shift which confirms that the 962-cm^{-1} band arises from the ν_1 mode of the PO_4 group.

The two major ν_3 bands at 1087 and 1046 cm^{-1} shifted 23 and 34 cm^{-1}, respectively, to lower frequencies, and the ν_4 bands at 601 and 571 cm^{-1} shifted 23 and 24 cm^{-1}, respectively, to lower frequencies. The frequencies of the fine structure in these bands arising from the isotopically different phosphate groups were not resolved. The maxima of the ν_3 and ν_4 bands is assumed to correspond primarily to the most abundant isotopic group, $P(^{16}O)(^{18}O)_3$, in this apatite as estimated from the ν_1 band areas. The ν_3 and ν_4 shifts for the $P(^{16}O)(^{18}O)_3$ group should roughly correspond to three-fourths of the band shifts for the $P(^{18}O)_4$ group. Using this approximation gives $P(^{18}O)_4$ frequency shifts of 31 and 45 cm^{-1} for the major ν_3 components and 32 cm^{-1} for each of the ν_4 components. Using the averages of the $P(^{16}O)_4$ bands at 1087, 1046 and 601, 571 cm^{-1} and the averages of the corresponding estimated $P(^{18}O)_4$ bands at 1056, 1001 and 569, 539 cm^{-1} gives a product ratio of (1028)(554)/(1066)·(586) = 0.912, which is in fair agreement with the predicted $\omega^i_3\omega^i_4/\omega_3\omega_4$ value of 0.924.

The weak Ca(OH)A band at 474 cm^{-1} shifted to 451 cm^{-1}. This frequency shift (23 cm^{-1}) which is close to that calculated (20 cm^{-1}) for the ν_2 mode of the $P(^{16}O)(^{18}O)_3$ group is good evidence that this band may arise from the ν_2 mode; additional data will be given to support this assignment. Assignment of the Ca(OH)A band at 474 cm^{-1} to a $\nu_3 - \nu_4$ difference tone[7,14-16] can be ruled out since replacement of ^{16}O by ^{18}O shifts ν_3 and ν_4 by approximately the same amounts. Thus, if the band at 474 cm^{-1} were a difference band, it would not shift as much as was observed. Also, difference bands are temperature dependent and decrease in

(11) J. C. Elliott, Ph.D. Thesis, University of London, 1964.
(12) J. E. Rosenthal, *Phys. Rev.*, 46, 730 (1934).
(13) G. Herzberg, "Infrared and Raman Spectra of Polyatomic Molecules," Van Nostrand, Princeton, N. J., 1964, p 235.
(14) V. M. Bhatnagar, *Bull. Soc. Chim. Fr., Spec.*, 1772 (1968).
(15) V. M. Bhatnagar, *Experientia*, 23, 10 (1967).
(16) V. M. Bhatnagar, *Chim. Anal. (Paris)*, 49, 406 (1967).

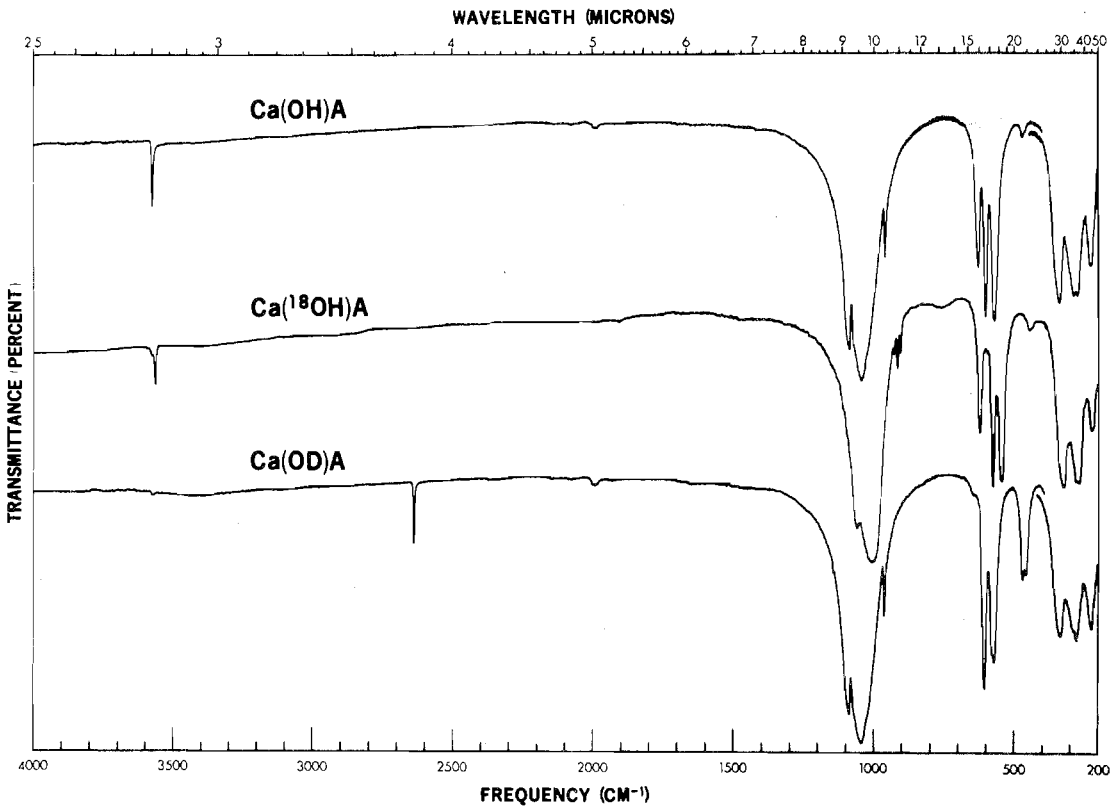

Figure 1. Infrared spectra of calcium OH, (^{18}OH, ^{18}O)-enriched, and OD apatites from 4000 to 200 cm^{-1} at 48°. The maxima of the most intense bands near 1000 cm^{-1} are at about 10% transmittance, and the base lines at 750 cm^{-1} are at about 90% transmittance.

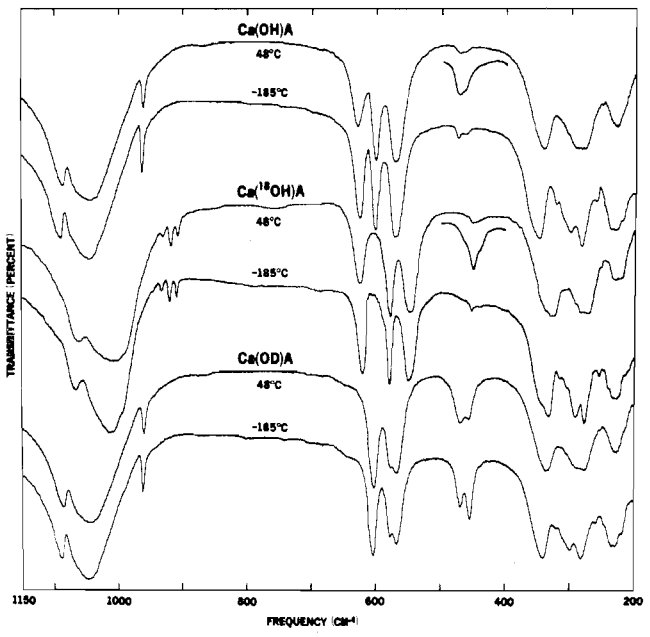

Figure 2. Infrared spectra of calcium OH, (^{18}OH, ^{18}O)-enriched, and OD apatites from 1150 to 200 cm^{-1} at 48 and −185°.

intensity upon lowering the temperature. The intensity of the band at 474 cm^{-1} does not decrease at −185° (Figure 2) which further rules out its assignment to a difference tone.

The frequencies at −185° of the major band near 350 cm^{-1} for the solid-state hydrothermal ^{40}Ca(OH)A preparation and the hydrothermally treated precipitated ^{40}Ca(OH)A preparation differ by about 5 cm^{-1} (Tables IV and V). At −185°, the solid-state hydrothermal ^{40}Ca(OH)A band maximum occurs at 349 cm^{-1} and the hydrothermally treated precipitated ^{40}Ca(OH)A band maximum occurs at 354 cm^{-1} whereas the band centers at half the band height are separated by about 2 cm^{-1}. At 48°, this band in both ^{40}Ca(OH)A preparations has a shoulder at about 355 cm^{-1} which shifts to about 363 cm^{-1} at −185° in the solid-state hydrothermal preparation and is not evident in the hydrothermally treated precipitated preparation at −185°. At 48°, the shoulder at 355 cm^{-1} appears to shift to lower frequency along with the band at 343 cm^{-1} on deuteration. The shoulder at 355 cm^{-1} is more evident particularly in precipitated preparations, indicating that the combined absorption band with the center near 345 cm^{-1} is actually a doublet composed of bands at 355 and 343 cm^{-1} which vary in intensity. Variation in intensity of each component can cause the band maximum to shift slightly which appears to be the reason for the slight differences in this band maximum between the solid-state and precipitated Ca(OH)A samples. Although the band maxima near 350 cm^{-1} differ for the solid-state and precipitated ^{40}Ca(OH)A series, this difference does not invalidate the relative frequency shifts on isotopic substitution in each series of preparations.

A $\nu_1 - \nu_4$ difference band (962 − 601 = 361 cm^{-1}) would also occur near the frequency of the shoulder. The lack of definite residual absorption at 355 cm^{-1} in the deuterated Ca(OH)A does not support assignment to a difference tone whereas the decrease in intensity of this shoulder at −185° is consistent with a difference tone. However, the shift in this band on deuteration is considered stronger evidence against its being a difference tone than is the decrease in intensity on cooling for a difference tone.

The low-frequency Ca(OH)A bands at 343, about 282, and 228 cm^{-1} all shift to lower frequency on ^{18}O, ^{44}Ca, and ^{48}Ca enrichment which establishes that both oxygen and Ca motions are involved in these vibrations. The band frequencies above 360 cm^{-1} for the hydrothermally treated precipitated ^{40}Ca-, ^{44}Ca-, and ^{48}Ca(OH)A, Figure 3, were

Table IV. Infrared Frequencies (cm^{-1}) and Assignments for Calcium OH-, OD-, and ^{18}O-Enriched Apatite[a] from 4000 to 200 cm^{-1} at 48 and −185°

Band freq							Isotopic freq shifts for $P^{16}O_{4-n}{}^{18}O_n$ modes				
48°			−185°					Internal		External	
Ca(OH)A	Ca(OD)A	Ca(^{18}OH)A	Ca(OH)A	Ca(OD)A	Ca(^{18}OH)A	Approx band shifts at −185°	n	Obsd	Calcd	Obsd	Band assignments
3572		~3574 sh	3575		~3578 sh						OH
	2636			2639		+3					OD str
		3563			3567						^{18}OH
1087	1086	1063	1090	1090	1067						
~1072 sh[f]	~1072 sh		~1075 sh	~1072 sh		+3	3[d]	23, 34			
1046	1046	1012	1049	1049	1015						$\nu_3(PO_4)$
~1032 sh	~1032 sh	~990 sh	~1035 sh	~1035 sh	~992 sh						
962	962		964	964			0				
		(945)[b]					1	17	14		
		932			934	+2	2	30	28		$\nu_1(PO_4)$
		919			921		3	43	41		
		908			910		4	54	55		
630			627								OH
	465[c] 469, 457			463[c] 470, 455		−3					OD lib
		627			623						^{18}OH
601	603	578	602	604	579		3[d]	23, 24			
571	578	547	571	578	547	0 to +1					$\nu_4(PO_4)$
	570			570							
~474	~469 sh		475				0				
~462 sh			463 sh								
						+1	1		7		
							2		14		
		451			452		3	23	20		$\nu_2(PO_4)$
		~442 sh			~442 sh		4		27		
~355 sh											
343		~345	349		~348 sh	+6					OH
	336			342							OD $(Ca_{II})_3$-X[e] "str"
		328			333						^{18}OH
			323 sh	322 sh	316 sh					7	
			~310 sh	~310 sh	~305 sh					~5	
~290	~290	~285	300	300	292	+5 to +10				8	Ca-PO_4 lattice modes
~275	~275	~270	283	283	277					6	
			261 sh	260 sh	254 sh					7	
~228	~228	~222	~234	~232	~227					~7	

[a] Solid-state hydrothermal apatite preparations. [b] Observed in samples containing less ^{18}O. [c] Band center. [d] Estimated most abundant value of n. [e] X = OH, OD, ^{18}OH. [f] sh = shoulder.

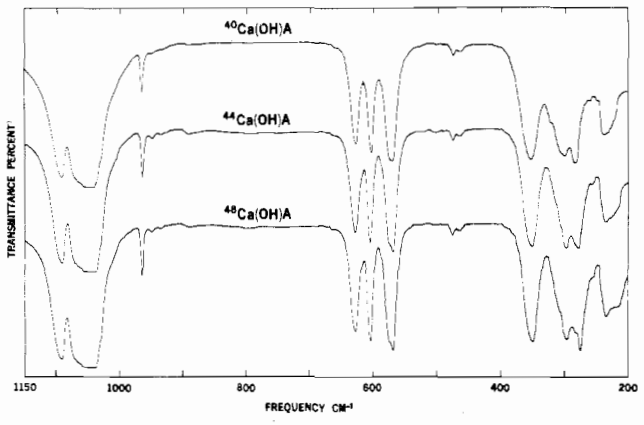

Figure 3. Infrared spectra of hydrothermally treated precipitated calcium-40, -44, and -48 hydroxyapatites from 1150 to 200 cm^{-1} at −185°. Spectra in the 1050-cm^{-1} region are at 0% transmittance.

Table V. Infrared Frequencies (cm^{-1}) for Calcium-40, -44, and -48 Hydroxyapatite[a] from 400 to 200 cm^{-1} at −185°

^{40}Ca(OH)A	^{44}Ca(OH)A[b]	Band shift	^{48}Ca(OH)A[c]	Band shift
354	352	−2	350	−4
~322 sh[d]				
~307 sh				
300	298	−2	296	−4
284	280	−4	275	−9
~260 sh	~256 sh	~−4	~254 sh	~−6
~235	~232	~−3	~230	~−5

[a] Hydrothermally treated precipitated apatite preparations. [b] 94% of total Ca as ^{44}Ca. [c] 78% of total Ca as ^{48}Ca. [d] sh = shoulder.

essentially the same (within 0.2-~1 cm^{-1}). At −185° the major Ca(OH)A band at about 282 cm^{-1} splits into a doublet, giving bands at 300 and 283 cm^{-1}, and additional weak shoulders are resolved (Figure 2 and Table IV) which are sensitive to the masses of the oxygens and Ca (Table V). The frequency shifts were measured from spectra recorded at −185° because the bands were resolved which reduced uncertainty in frequency readings. In the ^{18}O-enriched apatite, the band at 349 cm^{-1} shifted 16 cm^{-1} to lower frequency which is close to the calculated amount for either the ν_2 P(^{16}O)(^{18}O)$_3$ vibration (15 cm^{-1}) or for independent ^{18}OH translational motion (19 cm^{-1}) which will be discussed later. The major bands at 300 and 283 cm^{-1} shifted about 7 cm^{-1} on ^{18}O enrichment which is less than the predicted shift (12 cm^{-1}) for the ν_2 P(^{16}O)(^{18}O)$_3$ vibration. On the basis of the ^{18}O frequency shifts either of the bands at 474 or 343 cm^{-1} can be ascribed to the ν_2 vibration; additional information is given in the next sections to discern the assignments.

Hydroxyl Modes in OD-, ^{18}O- and ^{48}Ca-Enriched Apatite. Site and factor group symmetry analyses predict one infrared-active internal OH stretching mode and one infrared-active OH librational mode for Ca(OH)A (Tables I and III). The predicted decrease in the internal OH stretching frequency on D or ^{18}O substitution is given by $\nu^i = \nu(\mu/\mu^i)^{1/2}$, where μ is the reduced mass of the ion and i denotes the isotopic mass of frequency. For the external OH modes, in the limit of vanishing intermolecular forces, the predicted frequency decrease on D or ^{18}O substitution for the librational mode is given by $\nu^i = \nu(I/I^i)^{1/2}$ and for the translational mode by $\nu^i = \nu(M/M^i)^{1/2}$, where I is the moment of inertia and M is the total mass of the ion.[17] The reciprocal ν/ν^i ratios are given in Table VI.

(17) E. B. Wilson, Jr., J. C. Decius, and P. C. Cross, "Molecular Vibrations," McGraw-Hill, New York, N. Y., 1955, p 184.

Table VI. Observed and Calculated Frequency[a] Shifts and Ratios for Hydroxyl Modes in OD- and ^{18}OH-Enriched Apatite

	Str		Lib		Trans	
Apatite	Obsd	Calcd	Obsd	Calcd	Obsd	Calcd[d]
Ca(OD)A	936[b]	974	164	171	7	10
	1.355[c]	1.374	1.354	1.374	1.020	1.029
Ca(^{18}OH)A	8	12	4	2	16	19
	1.002	1.003	1.006	1.003	1.048	1.057
Sr(OD)A	943	979	130	145	15	9
	1.356	1.374	1.324	1.374	1.048	1.029
Ba(OD)A	946	983	95	114	19	8
	1.355	1.374	1.294	1.374	1.069	1.029

[a] Frequencies (cm^{-1}) at −185° used for data. [b] Frequency shifts. [c] OH:(^{18}OH, OD) frequency ratios. [d] Independent.

In Ca(OH)A the OH stretching (3572 cm^{-1}) and librational (630 cm^{-1}) bands are readily identified by the frequency shifts for the Ca(OD)A and Ca(^{18}OH)A analogs of nearly the calculated values (Table VI). The alternative assignment[6] of the Ca(OH)A band at 630 cm^{-1} to a Fermi resonance effect rather than to the OH librational mode can be ruled out because of the observed OD and ^{18}OH isotopic band shifts. The OD librational mode is centered at 465 cm^{-1} with bands at about 469 and 457 cm^{-1}; this splitting is better resolved at −185°. The weak Ca(OH)A band at 474 cm^{-1} and shoulder at 462 cm^{-1} occur close to the frequency of the OD librational mode; however, the intensity, especially at −185°, of the Ca(OD)A band at 469 cm^{-1} is greater than that expected for summation of the 474- and 462-cm^{-1} bands, and only a weak shoulder would be expected with a maximum a few reciprocal centimeters below 474 cm^{-1}. Since these bands occur at similar frequencies, vibrational coupling may account for the increased intensity of the band at 469 cm^{-1}. On the other hand, this OH mode is doubly degenerate and the two bands at 469 and 457 cm^{-1} could also arise from removal of degeneracy. If this is the case, an OD site symmetry less than C_3 would be required. A reduction in C_3 site symmetry is readily accomplished by a shift of the OD ion or deuteron off the C_3 axis closer to one of the Ca ions, resulting in C_1 site symmetry for the OD ion and removal of the degeneracy. If the site symmetry of the OD ion in Ca(OD)A is less than C_3 (*i.e.*, C_1), changes in vibrational modes of the 2[(Ca_{II})$_3$-(OD)] sublattice are also expected. One of these sublattice modes for Ca(OH)A at 343 cm^{-1} (assigned later) does not show the expected increased splitting or broadening on deuteration for a considerable shift of the OD ion off the C_3 axis; however, a slight tilt of the ion (deuteron off C_3 axis) should have little effect on this mode.

The ν_3 and ν_1 internal PO_4 vibrations in Ca(OH)A and Ca(OD)A occur at essentially the same frequencies. The lower frequency ν_4 PO_4 component at 571 cm^{-1} in this hydrothermally prepared Ca(OH)A does not show well-resolved splitting at 48 or at −185°, although three or more separate ν_4 frequencies are predicted. The corresponding band in CaFA, also poorly resolved in powder spectra,[18] is clearly resolved into two components in polarized infrared spectra of single crystals.[18,19] Similarly, the 571-cm^{-1} band in spectra of powdered Ca(OH)A is probably composed of at least two separate frequencies. The frequencies and intensities of the ν_4 components of Ca(OD)A differ slightly from those of Ca(OH)A. On deuteration, the Ca(OH)A band centered at 571 cm^{-1} separates into a doublet with maxima at 578 and 570 cm^{-1}

(18) E. Klein, J. P. LeGeros, O. R. Trautz, and R. Z. LeGeros, "Developments in Applied Spectroscopy," Plenum Press, New York, N. Y., 1970, p 13.

(19) L. C. Kravitz, J. D. Kingsley, and E. L. Elkin, *J. Chem. Phys.*, 49, 4600 (1968).

and the 601-cm^{-1} band shifts to 603 cm^{-1}. The areas of the Ca(OD)A band at 603 cm^{-1} and the doublet centered at 574 cm^{-1} are about 1.5 and 0.8 times, respectively, the areas of the corresponding bands in Ca(OH)A. These intensity changes and increased splitting of the ν_4 PO_4 modes are consistent with a more asymmetric PO_4 environment in Ca(OD)A.

Elliott[20] has indicated that a monoclinic form of Ca(OH)A may exist whose structure, by analogy with monoclinic chlorapatite,[21] would have PO_4 ions on three nonequivalent C_1 sites. The increased splitting of the ν_4 PO_4 mode and the OD librational mode in Ca(OD)A could also arise from a lower symmetry monoclinic structure. However, spectral differences were not detected for all the Ca(OD)A modes which argues against this. Lack of consistency throughout the Ca(OD)A spectrum for a considerably shifted OD position and/or lower unit cell symmetry suggests that differences observed for the ν_4 PO_4 and OD librational modes arise from interactions with other modes coincident with deuteration (*e.g.*, for Ca(OD)A, the 336 + 235 cm^{-1} combination interacting with the 571-cm^{-1} band and the (2 × 235)-cm^{-1} and/or the 474- and 462-cm^{-1} bands interacting with the OD librational band centered at 465 cm^{-1}. However, the possibility remains that the Ca(OD)A doublet at 469 and 457 cm^{-1} arises from a deuteron position off the C_3 axis.

In the 400-200-cm^{-1} region of Ca(OH)A only the band at 343 cm^{-1} definitely shifts on deuteration; the band at about 228 cm^{-1} appears to shift slightly, about 2 cm^{-1}, on deuteration. The Ca(OH)A band at 343 cm^{-1} shifted (7 cm^{-1}) to 336 cm^{-1} which is near to the value (10 cm^{-1}) predicted for independent translational motion of the OD group. In the ^{18}O enriched Ca(OH)A, the 343-cm^{-1} band shifted (15 cm^{-1}) to 328 cm^{-1} as compared to the calculated shift of 19 cm^{-1} for independent translational motion of the ^{18}OH group. However, this translatory motion of the OH group is not independent of the intermolecular forces; the frequency decreases of about 2 and 4 cm^{-1}, respectively, in the Ca(OH)A band at 343 cm^{-1} on ^{44}Ca and ^{48}Ca enrichment establish that Ca motion is also involved in this mode (Table V).

The modes involving translatory motions of the OH ions will be considered in terms of the 2[$(Ca_{II})_3$-(OH)] sublattice, although both Ca_I and PO_4 translations may also be involved in these modes. Twenty-four of the 54 translatory lattice modes in Ca(OH)A derive from the two [Ca_3-(OH)] groups. The forces within each Ca_3-(OH) group are certainly stronger than those between the two [Ca_3-(OH)] groups; consequently, the 2[Ca_3-(OH)] sublattice frequencies are expected to derive from the "internal" modes of the Ca_3-(OH) groups and coupling between modes of the two [Ca_3-(OH)] groups, if significant, will give rise to the factor group frequencies. Table VII classifies the "internal" and external modes of the 2(Ca_3-X) sublattices (X = F, OH) in Ca(OH)A and CaFA according to those derived from the isolated trigonal groups. The species and number of factor group modes derived from the 2(Ca_3-X) sublattice (Table VII) and those derived from the 6Ca_{II}, 2X translations (*i.e.*, from the factor group species of the 6 Ca_{II} and 2 X ions; Tables I and II) are the same. Eight coincident infrared- and Raman-active and four noncoincident Raman-active factor group modes derive from the 2[Ca_3-(OH)] sublattice whereas five infrared-active and six noncoincident Raman-active factor group modes derive from the 2(Ca_3-F) sublattice in CaFA (Table VII).

The observed isotopic frequency shift data will be compared with predicted shifts for geometric models in order to characterize the mode of the 2[Ca_3-(OH)] sublattice giving rise to the band at 343 cm^{-1}. The Ca_3-(OH) group has C_{3v} symmetry and occupies a C_3 site in Ca(OH)A. Disregarding the polar moment of the OH ion (the ion considered as a single atom) and its slight displacement from the trigonal Ca plane, the local Ca_3-(OH) geometry approximates D_{3h} symmetry. The highest frequency and strongest absorption expected and observed for a XY_3 group of D_{3h} symmetry (where mass of X < mass of Y) is the doubly degenerate antisymmetric X-Y stretch (ν_3) which would correspond to Ca_3-(OH) stretching motion perpendicular to the c axis in Ca(OH)A. Motion of the Ca_3-(OH) group parallel to the c axis would correspond to the out-of-plane bending mode (ν_2) of the planar XY_3 group; this mode should be lower in frequency and weaker in intensity than ν_3. The corresponding ν_4 mode would be lower in frequency than ν_2, and the ν_1 mode would be infrared inactive. The frequency shifts for the ν_1 and ν_2 modes of the isotopically substituted XY_3 (D_{3h} symmetry) group can be predicted directly from the isotopic masses whereas the ν_3 and ν_4 isotopic frequencies are combined in a $\nu_3\nu_4$ product shift.[22] However, when isotopically substituted $^{10}BX_3$ (D_{3h} symmetry; X = F, Cl, Br, I) is compared with $^{11}BX_3$, the experimentally observed frequency (frequencies tabulated and referenced in ref 23) ratios for ν^i_2/ν_2 and ν^i_3/ν_3 were nearly the same (within 0.5%). This is consistent with the predicted isotopic shifts because for central atom substitution[24] $\nu^i_2/\nu_2 = \nu^i_3\nu^i_4/\nu_3\nu_4$ and in the above series the observed ν_4 frequency is only slightly affected by a small increase in mass of the central atom. Using the approximations that the Ca_3-(OH) group has D_{3h} symmetry, that the OH group is a single atom, and that $\nu^i_2/\nu_2 \approx \nu^i_3/\nu_3$, the calculated and observed frequency shifts (cm^{-1}) for the 349-cm^{-1} band for either ν_2 or ν_3 type motion of the Ca_3-(OH) groups on isotopic substitution of the central atom are as follows: $^{40}Ca_3$-(^{16}OD), 9 (calcd), 7 (obsd); $^{40}Ca_3$-(^{18}OH), 16 (calcd), 16 (obsd). For ν_2 type motion on isotopic cation substitution the values are as follows: $^{44}Ca_3$-(^{16}OH), 2 (calcd), 2 ± 0.5 (obsd); $^{48}Ca_3$-(^{16}OH), 3.7 (calcd), 4 ± 0.5 (obsd). The ν_3 type shift is not estimated for isotopic cation substitution; however the ν_3 shift would be expected to be greater than that predicted for ν_2 type motion. The agreement between the approximated and observed frequency shifts is consistent with ν_3 or ν_2 type motion of the Ca_3-(OH) model on isotopic anion substitution and ν_2 type motion on isotopic cation substitution. As mentioned above the ν_3 type motion is expected to be both higher in frequency and stronger in intensity than the ν_2 type motion and consequently the Ca(OH)A band at 349 cm^{-1} probably arises from Ca_3-(OH) motion approximately perpendicular to the c axis which polarization measurements will confirm or establish as motion parallel to the c axis.

Klein, *et al.*,[18] reported that the transition moment for the CaFA infrared mode absorbing at about 336 cm^{-1} is perpendicular to the c axis. This band is assigned in a later section to Ca_3-F stretching (rather than to the ν_2 PO_4 mode[18]); the observed transition moment direction is consistent with in-plane ν_3 type stretching of the Ca_3-F groups.

The Raman shift[25] corresponding to the ν_3 type mode of the Ca_3-(OH) groups occurs at 329 cm^{-1}, 14 cm^{-1} lower than the infrared frequency. According to the selection rules for the 2(Ca_3-X) sublattices of Ca(OH)A and CaFA (Table VII),

(20) J. C. Elliott, *Nature (London) Phys. Sci.*, 230, 72 (1971).
(21) J. S. Prener, *J. Electrochem. Soc.*, 114, 77 (1967).
(22) Reference 13, p 178.
(23) K. Nakamoto, "Infrared Spectra of Inorganic and Coordination Compounds," Wiley, New York, N. Y., 1963, p 90.
(24) Reference 13, p 298.
(25) B. O. Fowler, unpublished results.

Table VII. Correlation Diagram and Spectral Activity for Sublattice Modes[a] of $Ca_{10}(PO_4)_6(OH)_2$ and $Ca_{10}(PO_4)_6F_2$

Apatite sublattice	Mode	Point group symmetry	Site group symmetry	Factor group symmetry
		C_{3v}	C_3	C_6
$2[(Ca_{II})_3\text{-}(OH)]$	Trans, ν_1, ν_2	$A_1(I, R)$	$A(I, R)$	$A(I, R) + B(0)$
	Lib	$A_2(0)$		
	Lib, trans, ν_3, ν_4	$E(I, R)$	$E(I, R)$	$E_1(I, R) + E_2(R)$
		D_{3h}	C_{3h}	C_{6h}
$2[(Ca_{II})_3\text{-}F]$	ν_1	$A_1'(R)$	$A'(R)$	$A_g(R) + B_u(0)$
	Lib	$A_2'(0)$		
	Trans, ν_2	$A_2''(I)$	$A''(I)$	$B_g(0) + A_u(I)$
	Trans, ν_3, ν_4	$E'(I, R)$	$E'(I, R)$	$E_{2g}(R) + E_{1u}(I)$
	Lib	$E''(R)$	$E''(R)$	$E_{1g}(R) + E_{2u}(0)$

[a] The ν_1, ν_2, ν_3, and ν_4 mode classification corresponds to internal modes of the isolated trigonal Y_3X group. The (OH) ion is considered as a single atom in the Ca_3-(OH) group. I = infrared active; R = Raman active; 0 = inactive in both infrared and Raman spectra.

these noncoincident infrared and Raman frequencies indicate that these modes originate from coupled ν_3 type modes of the two Ca_3-(OH) groups according to C_{6h} factor group symmetry which ignores the heteronuclearity and displacement of OH ion.

The ν_3 type motion of the $2[Ca_3\text{-}(OH)]$ sublattice is doubly degenerate and only one infrared-active ν_3 type band is predicted by factor group analysis. As pointed out above, spectra of Ca(OH)A at 48° have two bands at about 355 and 343 cm^{-1}. The weak 355-cm^{-1} band appears to shift along with the major 343-cm^{-1} band on deuteration; thus the 355-cm^{-1} band is also assigned to $2[Ca_3\text{-}(OH)]$ sublattice ν_3 type motion. Each of the Ca ions of the Ca_3-(OH) group are irregularly coordinated to six PO_4 oxygens, and Ca-OPO_3 interactions could easily account for splitting of this band.

The only other band in the 400–200-cm^{-1} region which shows indication of shifting on deuteration (2 cm^{-1}) is the poorly resolved band at about 234 cm^{-1}. This band at −185° appears to be composed of several bands and because of poor instrumental response in the 230–200-cm^{-1} region only the frequency of the band maxima was estimated. According to the Ca_3-(OH) model, if the 234-cm^{-1} band or a component of it arises from ν_2 type motion of the $2[Ca_3\text{-}(OH)]$ sublattice, the predicted shift on deuteration is 6 cm^{-1}, compared to the observed (2 cm^{-1}), and on ^{44}Ca and ^{48}Ca substitution, the observed shifts appear to be about twice the predicted shifts. However, because this band appears to be composed of several unresolved bands, shifts on isotopic substitution could not be determined with certainty.

Band Intensity. The infrared-inactive ν_1 and ν_2 modes of the undistorted tetrahedral phosphate group become active when the phosphate group is distorted to specific symmetries less than T_d. The small dipole moment changes that occur during both the ν_1 and ν_2 vibrations in slightly distorted phosphate groups give rise to infrared bands of weak intensity. The combined area of the Ca(OH)A bands originally assigned to the ν_2 PO_4 mode at about 343[5,6,14] and 282 cm^{-1} [6,14] is approximately 20 times the area of the ν_1 band at 962 cm^{-1}. To establish an approximate ν_1-to-ν_2 band intensity relationship for the distorted PO_4 group, compounds containing HPO_4 groups (C_{3v} symmetry or less), for which both the ν_1 and ν_2 modes are infrared active, were examined. The areas of the bands assigned to ν_2 in $CaHPO_4$,[26] $SrHPO_4$,[25] and $BaHPO_4$[27] were less than the areas of the bands corresponding to symmetric stretching of the HPO_4 groups. Thus, by analogy with the HPO_4 salts, the intensities of the Ca(OH)A bands at 343 and 282 cm^{-1} appear to be far too high to arise predominantly from the ν_2 PO_4 vibrations.

Studies by Hezel and Ross[28] of PO_4 ions on C_1 sites in a series of metal phosphate salts showed that the bands in the 490–460-cm^{-1} region that they assigned to ν_2 of the PO_4 group were considerably weaker in intensity than the intensities of the corresponding ν_1 PO_4 bands.

Calcium Hydroxyapatite Band Assignments in the 500–200-cm^{-1} Region. The Ca(OH)A bands in the 500–200 cm^{-1} region are assigned as follows. The weak band at 474 cm^{-1} and shoulder at about 462 cm^{-1} are assigned to the two components of the doubly degenerate internal ν_2 PO_4 bending mode because (a) the bands occurring at lower frequencies can be better ascribed to other vibrations, (b) the bands shifted approximately the correct amount on ^{18}O substitution for the ν_2 mode, (c) the intensities of these bands relative to the intensity of the ν_1 band are consistent with expectations, (d) the insensitivity of these frequency positions to changes in temperature and calcium mass is the expected behavior for a fundamental internal mode, and (e) the ν_2 mode should be infrared active in accord with the bands observed for the other internal PO_4 modes. This assignment is in agreement with previous infrared[8] and combined infrared and Raman[9,10] assignments for the internal ν_2 PO_4 mode.

The Ca(OH)A band at 343 cm^{-1} and shoulder at about 355 cm^{-1} are assigned to $2[Ca_3\text{-}(OH)]$ sublattice motion approximating Ca_3-(OH) ν_3 type stretching because of the expected shifts on D, ^{18}O, ^{44}Ca, and ^{48}Ca substitution. In accord with this assignment, the intensity of the 343-cm^{-1} band decreases concomitantly with decreases in the OH stretching and librational band intensities upon progressive dehydroxylation of Ca(OH)A.

The bands centered at about 290, 275, and 288 cm^{-1} are assigned to lattice modes involving concerted Ca and PO_4 motions because of the shifts on isotopic substitution. The additional weak shoulders observed in this region at −185° (Table IV) are also assigned to Ca-PO_4 lattice modes; however, some of these bands may arise from combinations with or overtones of lower frequency lattice modes and as already mentioned $2[Ca_3\text{-}(OH)]$ sublattice motion may also contribute to the poorly resolved band at about 228 cm^{-1}.

Six translatory and six libratory infrared-active C_6 factor group modes derive from the $6PO_4$ sublattice in Ca(OH)A (Table I); C_{6h} factor group analysis predicts half the above number of modes (Table II). The calculated frequency shifts at 300 cm^{-1} for independent translatory and rotatory motions of the $P(^{16}O)_4$, $P(^{18}O)_4$ isotopic pair are 12 and 17

(26) I. Petrov, B. Soptrajonov, N. Fuson, and J. R. Lawson, *Spectrochim. Acta, Part A*, 23, 2637 (1967).

(27) Ya. I. Ryskin and G. P. Stavitskaya, *Opt. Spectrosc. (USSR)*, 8, 320 (1960).

(28) A. Hezel and S. D. Ross, *Spectrochim. Acta*, 22, 1949 (1966).

cm^{-1}, respectively; for independent translatory motion of the $P(^{16}O)_4$, $P(^{16}O)(^{18}O)_3$ isotopic pair, 9 cm^{-1}; and for independent translatory motion of the ^{40}Ca, ^{44}Ca and ^{40}Ca, ^{48}Ca isotopic pairs, 15 and 26 cm^{-1}, respectively. The observed band shifts for the ^{18}O-enriched Ca(OH)A (containing the estimated most abundant isotopic group, $P(^{16}O)(^{18}O)_3$) in the 300-cm^{-1} region are about 7 cm^{-1}; these shifts are closer to those predicted for independent translatory type than for rotatory type PO_4 motion. All of the bands in this region are sensitive to isotopic Ca mass and display isotopic frequency shifts which are about 10-30% of the predicted shifts for independent translatory Ca motion. The Ca_{II} ions on C_1 sites are coordinated to six oxygen atoms and to the OH group; the Ca_I ions on C_3 sites are coordinated to nine oxygen atoms, with Ca-O bond lengths ranging from about 2.4 to 2.8 Å.[29] Since the Ca-O bonding is thought to be ionic, no internal Ca-O type modes are expected. The minor frequency shifts on isotopic calcium substitution in this region point either to minimal calcium motion in these modes or more probably to the multiple phosphate oxygen to calcium coordination which effectively reduces the calcium mass during these vibrations.

Comparison between Observed and Predicted Bands. 1. Internal Modes. The number of infrared frequencies observed for each internal PO_4 mode of Ca(OH)A, Table IV, agree better with site group analysis predictions (9 total frequencies) than with factor group analysis (18 total frequencies), Table III. Similarly, the number of Raman frequencies,[10] about 9, is more consistent with site group analysis whereas noncoincidence of most of the infrared and Raman frequencies[10] supports factor group predictions. However, for CaFA, both the observed number and noncoincidence of the infrared and Raman internal PO_4 frequencies[9,19,30] agree with factor group analysis. This argues that factor group coupling should similarly occur in Ca(OH)A. The large discrepancy between the observed and predicted number of infrared and Raman internal PO_4 frequencies for Ca(OH)A according to C_6 factor group analysis indicates that the OH ion and its slight displacement do not effectively reduce the overall C_{6h} lattice symmetry enough that C_6 factor group selection rules become operative. Thus, C_{6h} factor group selection rules better describe the observed infrared and Raman internal PO_4 frequencies of Ca(OH)A.[10]

The single infrared internal OH stretching frequency and single coincident (within 1 cm^{-1}) Raman frequency[10,25] agree with both site and factor group analyses (Table III).

2. Lattice Modes. Lack of spectral data below 200 cm^{-1} and incomplete assignments preclude complete comparison with the predicted number and types of lattice modes. However, low-temperature infrared spectra above 200 cm^{-1} display about eight lattice frequencies for Ca(OH)A. Of these, the predicted single infrared OH librational frequency was observed; corresponding Raman data are inconclusive.[10] One lattice frequency was attributed to a factor group mode of the $2[Ca_3\text{-}(OH)]$ sublattice according to C_{6h} symmetry. The majority of the other lattice frequencies above 200 cm^{-1} derive from concerted Ca-PO_4 modes possibly involving mostly PO_4 translatory motion.

About eight lattice frequencies are evident in the room-temperature infrared spectra[9] of powdered mineralogical Ca(OH)A and CaFA in the 375-60-cm^{-1} region. This number of Ca(OH)A lattice frequencies is markedly less than that predicted by C_6 factor group analysis (22; excluding the higher frequency OH librational mode) and is more in agreement with C_{6h} factor group predictions for CaFA (11 frequencies which ignore the lattice symmetry lowering by the OH ion). However, Figure 2 illustrates that low-temperature spectra of the powdered apatites are necessary to resolve the broad lattice modes and Table III shows that both infrared and Raman data are necessary to classify the apatite lattice modes. A combined low-temperature infrared and Raman study of these isotopically substituted apatites in the 400-30 cm^{-1} region will be given elsewhere.

Strontium and Barium Hydroxyapatite. The apatites Sr(OH)A and Ba(OH)A also crystallize in hexagonal lattices and are reported to be structurally very similar to Ca(OH)A (cited in a review by Mooney and Aia[31]). The structural positions of the OH ion along the c axis in Sr- and Ba(OH)A have not been established as they have in Ca(OH)A. These incomplete structural data preclude deriving the exact factor group vibrational selection rules. However, the vibrational selection rules for Ca(OH)A and CaFA (which disregard the heteronuclearity, position, and orientation of the OH ion) will be used as models for interpreting spectra of these structurally related analogs of the calcium apatites.

The internal phosphate modes of Sr(OH)A and Ba(OH)A were assigned by analogy with those of Ca(OH)A, and the OH modes, by shifts on deuteration. The frequencies of the lattice modes of these analogs of Ca(OH)A should be more sensitive to changes in cation mass and interionic forces than the fundamental internal modes of the PO_4 group. This dependency should aid in distinguishing between internal and lattice modes occurring at similar frequencies.

The Sr(OH)A band at 3592 cm^{-1} and the Ba(OH)A band at 3606 cm^{-1} are identified as the internal OH stretching modes, and the Sr(OH)A band at 535 cm^{-1} and the Ba(OH)A band at 430 cm^{-1}, as the OH librational modes from the shifts on deuteration (Figures 4 and 5; Tables VI and VIII).

The ν_3, ν_1, and ν_4 internal phosphate modes are readily assigned by comparison with those of Ca(OH)A (Table IV). The lower frequency ν_4 components centered at 566 cm^{-1} in Sr(OH)A and at 558 cm^{-1} in Ba(OH)A are well resolved, especially at $-185°$, as compared to the corresponding band in Ca(OH)A. On deuteration these ν_4 components do not show the intensity changes that are observed for Ca(OD)A.

In the 500-200-cm^{-1} region, Sr(OH)A has bands at 457, 323, and 240 cm^{-1}; Ba(OH)A has bands at 443, 430 (OH libration), and 284 cm^{-1} and the shoulder of a band at 200 cm^{-1} with its maximum at less than 200 cm^{-1}. The Sr(OH)A band at 323 cm^{-1} and the Ba(OH)A band at 284 cm^{-1} shift 11 and 19 cm^{-1}, respectively, to lower frequencies on deuteration and are assigned to modes involving OH translatory motion. These observed shifts are greater than the calculated shifts for independent OH translatory motion (Tables VI and VIII); this indicates slight proton rocking during translation of the OH group. The lattice dimension increase,[1] in the Ca-, Sr-, Ba(OH)A sequence, results in an increasingly open structure about the OH ions. A progressively less restraining crystal force field on the OH ions should permit increased mixing of the OH librational and translational motions with the resultant increase in the deviations from the calculated values. By analogy with the corresponding OH "translatory" mode in Ca(OH)A and assuming similar local M_3-(OH) structure in these analogs, these modes are expected to involve concerted motions of the cations and OH ions comprising the M_3-(OH) groups. The noncoincident

(29) A. S. Posner, A. Perloff, and A. F. Diorio, *Acta Crystallogr.*, 11, 308 (1958).

(30) W. E. Klee, *Z. Kristallogr., Kristallgeometrie, Kristallphys., Kristallchem.*, 131, 95 (1970).

(31) R. W. Mooney and M. A. Aia, *Chem. Rev.*, 61, 433 (1961).

Table VIII. Infrared Frequencies (cm^{-1}) and Assignments for Strontium and Barium OH and OD Apatites from 4000 to 200 cm^{-1} at 48 and −185°

Band freq									
48°				−185°				Approx band shifts at −185°	Band assignments
Sr(OH)A	Sr(OD)A	Ba(OH)A	Ba(OD)A	Sr(OH)A	Sr(OD)A	Ba(OH)A	Ba(OD)A		
3592		3606		3594		3609		+2	OH str
	2649		2661		2651		2663		OD str
1071	1071	1048	1048	1074	1074	1051	1051		
~1052 sh[c]	~1052 sh	~1030 sh	~1030 sh	~1055 sh	~1055 sh	~1033 sh	~1033 sh		
1030	1030	1012	1012	1033	1033	1015	1015	+3	$\nu_3(PO_4)$
~1018 sh	~1018 sh	~999 sh	~999 sh	~1021 sh	~1021 sh	~1002 sh	~1002 sh		
947	947	933	933	949	949	935	935	+2	$\nu_1(PO_4)$
535		~430		531	(~531 sh)	418	(418)[a]	−2 to ~−12	OH lib
	403		~328		401		323		OD lib
592	592	580	580	593	593	581	581		
572	570	561	561	573	570	562	562	0 to +1	$\nu_4(PO_4)$
563	563	556	556	563	563	557	556		
457	457	443	443	458	458	443	443	+1	$\nu_2(PO_4)$
				~453 sh					
323		284		330	(330)	293	(292)	+3 to +9	OH M_3-(OH, OD)
	312		265–275[b]		315		274		OD "str"
240	240	<200	<200	252	252	216	216	≧+6	Cation–PO_4 lattice modes
				239	239				

[a] Hydroxyl frequencies in spectra of incompletely deuterated apatites are in parentheses. [b] Exact frequency at 48° uncertain because of band broadness and incomplete deuteration. [c] sh = shoulder.

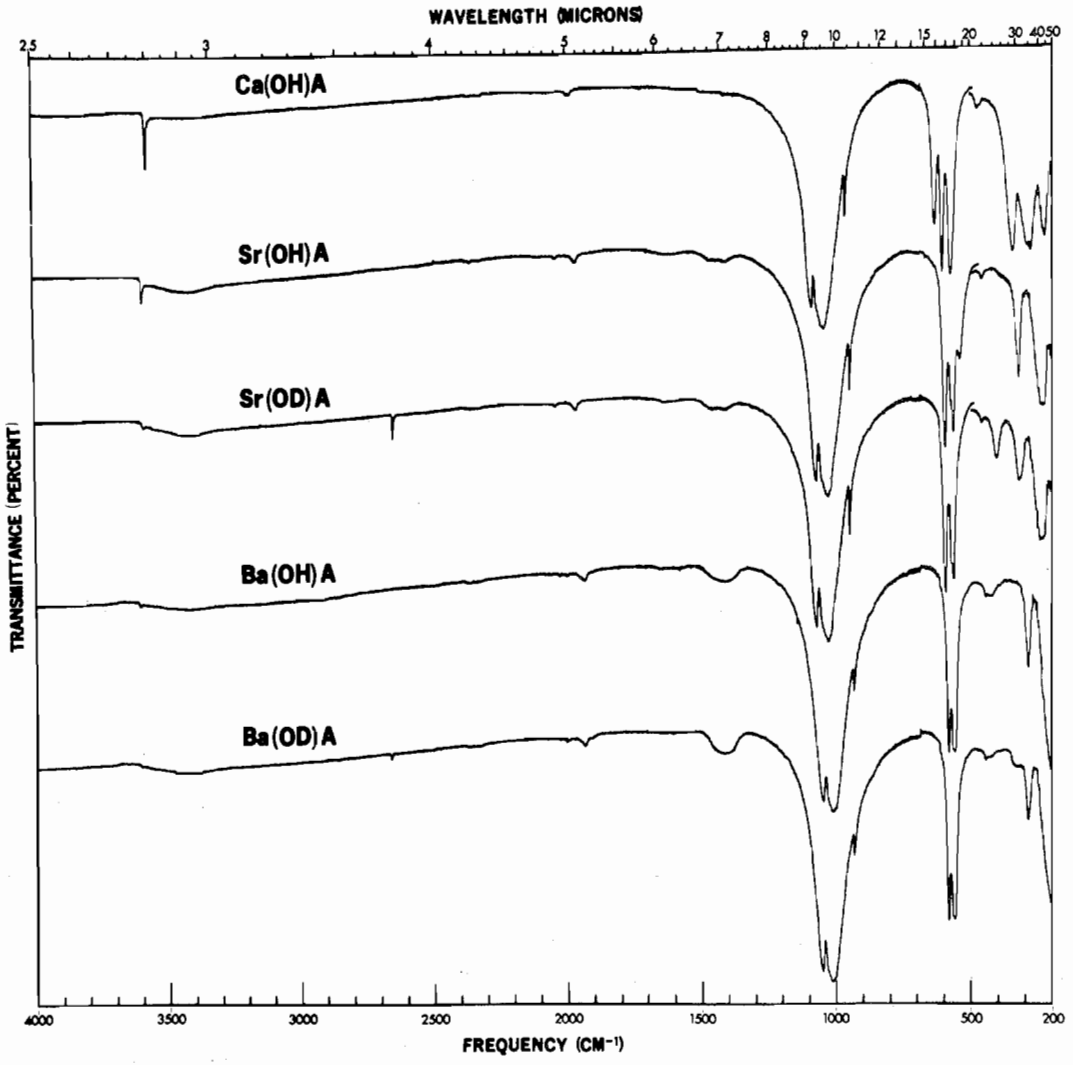

Figure 4. Infrared spectra of calcium OH apatite and strontium and barium OH and OD apatites from 4000 to 200 cm^{-1} at 48°. The broad bands at about 3450 and 1625 cm^{-1} arise from adsorbed water, and the bands at about 1500–1400 cm^{-1} arise from carbonate. These bands are not listed in the tables.

infrared (Sr(OH)A, 323 cm^{-1}; Ba(OH)A, 284 cm^{-1}) and Raman (Sr(OH)A, 308 cm^{-1}; Ba(OH)A, 273 cm^{-1}) frequencies[25] can be similarly ascribed, as for Ca(OH)A, to coupling between the two M_3-(OH) groups in the unit cell. The areas

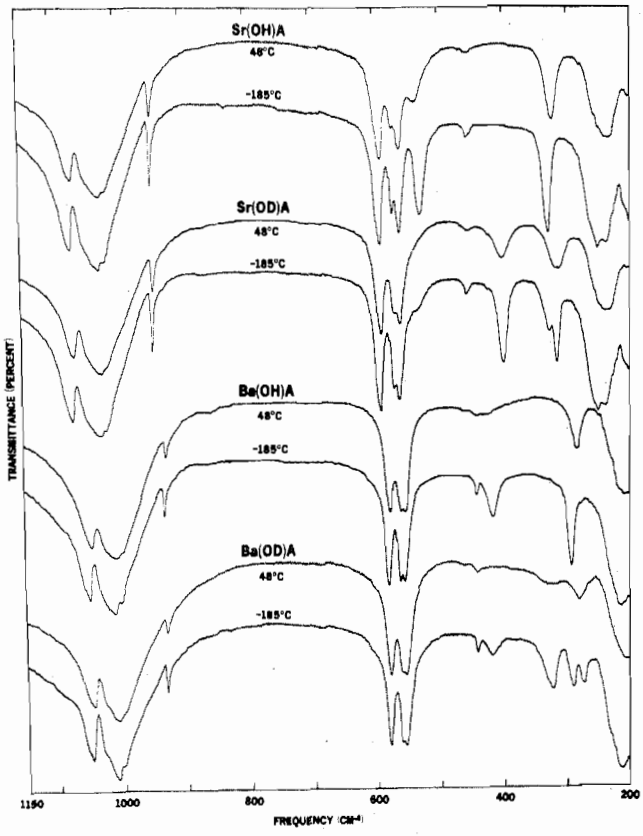

Figure 5. Infrared spectra of strontium and barium OH and OD apatites from 1150 to 200 cm^{-1} at 48 and −185°.

(from linear absorbance recordings) of the Sr(OH)A and Ba(OH)A bands at 323 and 284 cm^{-1}, respectively, are approximately 4 times the areas of their ν_1 bands, and the area of the Sr(OH)A band at 240 cm^{-1} is approximately 7 times that of its ν_1 mode. These band intensities are greater than those approximated for the ν_2 mode, again indicating that these bands do not arise from the ν_2 mode of the PO_4 group. The Sr(OH)A band at 457 cm^{-1} and shoulder at about 453 cm^{-1} and the Ba(OH)A band at about 443 cm^{-1} are assigned to components of the ν_2 PO_4 mode by analogy with both the similar frequencies and intensities of the ν_2 PO_4 bands in Ca(OH)A. The Sr(OH)A band at 240 cm^{-1} and Ba(OH)A band near 200 cm^{-1} are assigned to cation-PO_4 lattice modes again by analogy with those of Ca(OH)A and because of the progressively greater shifts in these frequencies compared to the shifts in the internal PO_4 frequencies which is expected for lattice modes.[1]

The basic structural similarities of Ca-, Sr-, and Ba(OH)A are evident from a comparison of the internal vibrational modes of the PO_4 ion in these apatites. The similarities in the ν_3 and ν_1 band shapes and intensities show that the PO_4 ion experiences similar environments which is in agreement with the reported structural similarity of these compounds.

The infrared assignments for the internal PO_4 modes of Sr(OH)A and Ba(OH)A agree with those previously given by Fowler[8] and Blakeslee and Condrate;[10] however, the latter investigators, utilizing combined infrared and Raman spectra, demonstrated coupling between several of the internal PO_4 modes.

The number of infrared-active internal PO_4 frequencies (about 9) observed for Sr(OH)A and Ba(OH)A shows that C_6 factor group selection rules are also not operative for these apatites (Tables III and VIII). However, the non-coincidence of most of the infrared and Raman internal PO_4 frequencies is consistent with factor group analysis rather than with site group analysis; thus, similarly as for Ca(OH)A, C_{6h} factor group selection rules better describe the internal PO_4 modes.[10]

The predicted single infrared OH stretching and librational frequencies were observed for each apatite. Also, the predicted single and coincident Raman OH stretching frequencies were observed at 3592 cm^{-1} for Sr(OH)A and at 3607 cm^{-1} for Ba(OH)A;[25] corresponding Raman data for the OH librational modes are inconclusive.[10] Blakeslee and Condrate[10] also reported coincident infrared and Raman OH stretching frequencies for Sr(OH)A at 3593 cm^{-1}; however, they reported the Ba(OH)A Raman OH stretching frequency occurs at 3527 cm^{-1} (as compared to 3607 cm^{-1} in the present study) and did not detect the 3606-cm^{-1} infrared frequency. The different Raman frequency reported by Blakeslee and Condrate[10] may arise from an impurity or possibly from a different ordering of OH ions in their Ba(OH)A.

Of the predicted eleven infrared-active lattice modes (excluding the OH librational mode) according to C_{6h} factor group analysis, three were observed for Sr(OH)A and two for Ba(OH)A above 200 cm^{-1} at −185° (Tables III and VIII).

Other Apatites. The band assignments for Ca-, Sr-, and Ba(OH)A are also common to other structurally related apatites, which, of course, include the biological apatites. Assignments for specific infrared bands of several apatites in the 500–200-cm^{-1} region, as based on the combined data given in this study, are as follows. The CaFA band at about 325 cm^{-1} is assigned to Ca_3-F "ν_3 type stretching" of the 2(Ca_3-F) sublattice by analogy with the corresponding band in Ca(OH)A at 343 cm^{-1} and because of the fact that the shift 343 to 325 cm^{-1} is nearly that calculated (16 cm^{-1}) for the larger mass of F over that of OH. No significant difference in Ca_3-F and Ca_3-(OH) bond strength is indicated because for the same composite anion mass (F and ^{18}OH), the Ca_3-F and Ca_3-(^{18}OH) "stretching" frequencies are nearly the same, 325 and 328 cm^{-1}, respectively. However, assignment and comparison of all vibrational frequencies (infrared and Raman) of the 2[Ca_3-(OH)] and 2(Ca_3-F) sublattices will afford a better basis for bonding comparison. Similarly, the CaFA band at about 474 cm^{-1} is assigned to the internal ν_2 PO_4 bending mode which is in accord with previous reassignments;[8,9] the doublet at about 280 cm^{-1} and part of the poorly resolved band at about 230 cm^{-1} are assigned to Ca-PO_4 lattice modes.

Analogous arguments for the lower frequency assignments should also apply for the Cl apatite of calcium and the F and Cl apatites of strontium and barium, taking into account the differences expected for the "translatory" type Cl motion because of the Cl positions between the adjacent Ca triads in Cl apatites.[21,32] Accordingly and in agreement with previous reassignments,[9] the calcium chloroapatite band at 472 cm^{-1} is assigned to the internal ν_2 PO_4 bending mode, and the major band at about 290 cm^{-1}, to lattice modes. Also, the apparently unreported strontium fluorapatite bands at 457, 317, and 235 cm^{-1} and the barium fluorapatite bands at 442, 286, and about 200 cm^{-1} are respectively assigned in each sequence to the internal ν_2 PO_4 bending mode and M_3-F "stretching" and cation-PO_4 lattice modes.[25]

Overtone, Combination, and Other Bands. The Ca(OH)A bands in the 2000-cm^{-1} region, Figures 4 and 6, have been assigned to $2\nu_3$ overtones, combinations of ν_3 components,

(32) R. A. Young and J. C. Elliott, *Arch. Oral Biol.*, 11, 699 (1966).

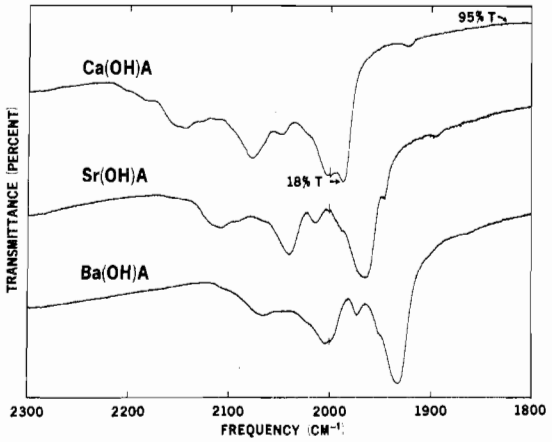

Figure 6. Infrared spectra of calcium, strontium, and barium hydroxyapatites from 2300 to 1800 cm^{-1} at 48°. The absorbances of these bands correspond to apatite sample concentrations about 60 times those of spectra shown in Figures 1 and 4.

and $\nu_3 + \nu_1$ combinations.[5,6,33] Eight additional extremely weak Ca(OH)A bands were detected in this region, and they are listed along with the major Ca(OH)A bands at 2145, 2078, 2048, 2003, and 1987 cm^{-1} in Table IX. Some of these bands can be assigned to either overtones or combinations, and these are indicated in Table IX. The corresponding Sr- and Ba(OH)A overtones and combinations occur at lower frequencies concomitant with the lower frequencies of the fundamentals.

Levitt and Condrate[34] and Klee[30] have reported polarized infrared spectra of single crystals of geological CaFA (from Durango, Mexico) which show the major bands in the 2000-cm^{-1} region. These investigators also observed weak bands for the geological CaFA (containing a trace of OH ions) in the OH stretching region at about 3535 cm^{-1} and a shoulder at about 3485 cm^{-1} and established that the vibrational transition moments for both modes are parallel to the crystal *c* axis. Klee[30] also reported numerous other weak bands, including bands at 740 and 710 cm^{-1}, assigned to combinations, having transition moments perpendicular and parallel to the crystal *c* axis, respectively. Corresponding bands at about 3535, 735, and 715 cm^{-1} (and additional bands at 3545 and 670 cm^{-1}) have been assigned in powdered synthetic $Ca_{10}(PO_4)_6F_{2-x}(OH)_x$, Ca(OH,F)A, apatites of controlled F and OH composition to OH stretching and librational modes of OH ions weakly hydrogen bonded to F ions along the column as based on combined data (deuterium sensitivity, hydrogen bond frequency shift criteria, band broadening, and OH band intensity–F content correlations).[8] The frequencies at about 735 and 715 cm^{-1} are average frequencies and they differ slightly from those given by Klee;[30] these frequencies and the 670-cm^{-1} frequency are about 5 cm^{-1} higher in F-rich and about 5 cm^{-1} lower in OH-rich Ca(OH,F)A.[25] Also, the number of frequencies and band intensity changes observed for the OH stretching and librational modes of the synthetic Ca(OH,F)A apatites were utilized to establish at least two nonequivalent OH- - -F bonds and preferential intermingling of OH and F ions along the columns rather than separate aggregation of each ion and to infer enhanced chemical stability of the OH- and F-containing apatite.[8,35] Young, van der Lugt, and Elliott[36] have demonstrated two nonequivalent OH- - -F interactions in geological Ca(OH)A containing F ions using nmr. The transition moments observed for the 3535-cm^{-1} band[30,34] and the 740-cm^{-1} band[30] of the geological CaFA agree with those expected for OH- - -F assignments[8] in the synthetic analogs; however, the transition moment for the very weak 710-cm^{-1} band[30] does not. This very weak geological CaFA band at 710 cm^{-1} may arise from other sources, *e.g.*, combinations[30] and/or CO_3 impurities. The intensities of the 735-, 715-, and 670-cm^{-1} librational bands of the synthetic Ca(OH,F)A vary as a function of OH and F contents: when F > OH, the 735-cm^{-1} band predominates; when OH > F, the 715- and 670-cm^{-1} bands predominate.[8] The corresponding bands and intensity trends are observed for geological apatites (CaFA from Durango, Mexico, and Ca(OH)A from Holly Springs, Ga.).[25] Hence, polarized infrared spectra of Ca(OH,F)A varying in OH and F contents, to achieve intensities significantly above those of possible interfering combination and CO_3 absorptions occurring in the 700-cm^{-1} region, are needed to identify unambiguously the transition moments of the 735-, 715-, and 670-cm^{-1} OH librational modes. Dykes and Elliott[37] have indicated that the band at about 3498 cm^{-1} in geological (Holly Springs, Ga.) and synthetic Ca(OH)A containing Cl arises from OH stretching of OH ions hydrogen bonded to Cl ions along the apatite column; this is near the 3485-cm^{-1} frequency observed for the geological CaFA.[30,34]

Baddiel and Berry[6] reported weak Ca(OH)A bands, which others have not reported, at 1208, 1185, 1154, and 950 cm^{-1} and assigned them to combinations or overtones, and they reported unassigned weak bands at 725 and 980 cm^{-1}. The frequencies of most of these bands agree with those of β-$Ca_2P_2O_7$.[5] Baddiel and Berry[6] ignited their Ca(OH)A sample at 580° and it is probable that a trace of β-$Ca_2P_2O_7$ formed on ignition as a result of acidic phosphate in the original material.

Bhatnagar[14,38] reported that the infrared spectra of Ca(OH)A usually have weak bands at about 425 cm^{-1}. This band was not reported by other investigators.[5,6,7,10,33] Spectra of numerous Ca(OH)A samples, some recorded in different suspension media (Nujol, KBr, CsI) or as pressed thin films, showed only the 474-cm^{-1} band and shoulder at about 465 cm^{-1} in the 500–400-cm^{-1} region. No definite

Table IX. Infrared Frequencies (cm^{-1}) at 48° and assignments for Calcium, Strontium, and Barium Hydroxyapatites from 2300 to 1800 cm^{-1}

Band freq			
Ca(OH)A	Sr(OH)A	Ba(OH)A	Band assignments
~2205	~2155	~2105	*a*
~2185			
~2155 sh[b]	~2120 sh	~2072 sh	$2\nu_3$ overtones and ν_3 combinations
2145	2109	2065	
~2128	~2091	~2045	
~2114	~2068	~2024	
2078	2041	2004	
~2068 sh			
2048	2014	1972	$\nu_3 + \nu_1$ combinations
~2024 sh	~1990 sh	~1951 sh	
2003	1965	1933	
1987	1945		
1923	1893	~1863	$2\nu_1$

[a] Possible $2\nu_3$ overtones or ν_3 combinations of undetected higher frequency ν_3 components. [b] sh = shoulder.

(33) L. Winand and G. Duyckaerts, *Bull. Soc. Chim. Belg.*, **71**, 142 (1962).
(34) S. R. Levitt and R. A. Condrate, *Appl. Spectrosc.*, **24**, 288 (1970).
(35) B. O. Fowler, Abstracts, 45th General Meeting of the International Association for Dental Research, Washington, D. C., March 16–19, 1967, No. 247.
(36) R. A. Young, W. van der Lugt, and J. C. Elliott, *Nature (London)*, **223**, 729 (1969).
(37) E. Dykes and J. C. Elliott, *Calcif. Tissue Res.*, **7**, 241 (1971).
(38) V. M. Bhatnagar, *Arch. Oral Biol.*, **12**, 165 (1967).

additional bands were observed in this region at −185° or by varying the Ca(OH)A particle size from 200 to 2 μ or by varying pellet formation pressures from 10 to 50 tons/in.^{2}.

Although $\nu_3 - \nu_4$ difference bands are allowed in the 520–400-cm^{-1} region, it is questionable whether the weak Ca(OH)A band at about 425 cm^{-1} reported by Bhatnagar[14,38] is characteristic of powdered samples of pure crystalline stoichiometric Ca(OH)A. However, a definite band is observed at about 435 cm^{-1} in the spectra of Ca(OH)A ignited under certain conditions. This band at about 435 cm^{-1} (not attributed to second phases of $Ca_3(PO_4)_2$ or $Ca_4(PO_4)_2O$) in the spectrum of partially dehydroxylated Ca(OH)A effected by thermal treatment may arise from vibrational motion of $Ca^{2+}{}_3$–O^{2-} groups along the column where the O^{2-} ion has replaced the OH^- ion.[25] Identification and assignment of this band utilizing isotopic calcium and oxygen will be given elsewhere.

Registry No. CFA, 1306-05-4; Ca(OH)A, 1306-06-5; Sr(OH)A, 12266-00-1; Ba(OH)A, 12356-34-2; D_2, 7782-39-0; ^{18}O, 14797-71-8; ^{44}Ca, 14255-03-9; ^{48}Ca, 13981-76-5; $Ca_5F(PO_4)_3$, 12015-73-5; $Ca_5(OH)(PO_4)_3$, 12167-74-7; $Sr_5(OH)(PO_4)_3$, 12195-53-8; $Ba_5(OH)(PO_4)_3$, 12377-63-8.

Contribution from the National Institute of Dental Research, National Institutes of Health, Bethesda, Maryland 20014

Infrared Studies of Apatites. II. Preparation of Normal and Isotopically Substituted Calcium, Strontium, and Barium Hydroxyapatites and Spectra–Structure–Composition Correlations

B. O. FOWLER

Received July 11, 1973

Procedures are described for preparation of calcium, strontium, and barium hydroxyapatites, their deuterated analogs, and calcium hydroxyapatite enriched with isotopic calcium with particular emphasis on purity, stoichiometry, crystal perfection, and gravimetrically monitoring the apatite composition. The effects of low temperature and differences in physical properties of the apatites on the infrared vibrational frequencies are discussed. Shifts in the internal phosphate modes to higher frequencies, in the barium–strontium–calcium hydroxyapatite sequence and also on cooling, are attributed primarily to increased interphosphate repulsion concomitant with lattice contraction. Causes for variation in the frequencies and intensities of the OH modes are considered from several viewpoints including the presence of weak OH- - -O bonding which is neither conclusively established nor rejected. Marked increases in OH band intensities in the barium–strontium–calcium hydroxyapatite sequence are attributed to differences in OH bonding rather than to other effects.

Introduction

Pure stoichiometric hydroxyapatites, $M_{10}(PO_4)_6(OH)_2$ (M = Ca, Sr, Ba), are difficult to prepare from solution. The precipitated calcium hydroxyapatite is usually nonstoichiometric with a Ca:P ratio less than theoretical and contains acid phosphate, carbonate, and excess water.[1] Precipitated nonstoichiometric calcium hydroxyapatites thermally annealed (*e.g.*, 900° in air) to reduce volatile impurities and increase crystallinity yield second phases of β-$Ca_3(PO_4)_2$ and CaO for Ca:P ratios less than and greater than 1.67, respectively.[2] The apatite nonstoichiometry and second phases can be minimized by direct thermal combination of the appropriate reactants in the solid state. The stoichiometry and purity of the solid-state apatite preparations are limited, primarily, only by the purity and stoichiometry of the reactants, provided sufficient time is allowed for thermal diffusion for reaction completion and there is no volatilization of essential components during ignition.

Hydrothermal bomb methods, employing restricted chemical compositions,[3] yield essentially single phases of well-crystallized calcium hydroxyapatite; however, specialized apparatus is required and quantities produced are usually small.

Procedures are described in this paper for solid-state preparation of calcium hydroxyapatite, Ca(OH)A, strontium hydroxyapatite, Sr(OH)A, barium hydroxyapatite, Ba(OH)A, mixed calcium–strontium hydroxyapatite, their deuterated analogs, and precipitated Ca(OH)A enriched with isotopic calcium, with particular emphasis on purity, stoichiometry, crystal perfection, and gravimetrically monitoring the apatite composition.

These apatite preparations were utilized in the preceding paper[4] for infrared vibrational assignments. The effects of low temperature and differences in physical properties of the apatites on the infrared frequencies and causes for hydroxyl frequency and intensity differences are considered in this paper.

Experimental Section

Apatite Preparations. 1. Calcium, Strontium, and Barium Hydroxyapatites. These apatites were prepared in the solid state according to the reactions[5]

$$2MHPO_4 \xrightarrow[\text{air}]{1000^\circ} M_2P_2O_7 + \overline{H_2O} \quad (1)$$

$$3M_2P_2O_7 + 4MCO_3 \xrightarrow[\text{vacuum}]{1100^\circ} 10MO{\cdot}3P_2O_5 + \overline{4CO_2} \quad (2)$$

$$10MO{\cdot}3P_2O_5 \xrightarrow[H_2O,\ 1.5\ \text{atm}]{900\text{–}1100^\circ} M_{10}(PO_4)_6(OH)_2 \quad (3)$$

The reactions were carried out in a controlled atmosphere in a tube inserted in a furnace. This apparatus consisted of a no. 310 stainless steel tube 18 in. long, with a $1^5/_8$-in. inside diameter and $^1/_8$-in. wall, closed on one end and threaded on the other to fit a brass cap. The cap was fitted with a Teflon gasket for sealing and had

(1) See W. E. Brown, *Clin. Orthop. Related Res.*, 44, 205 (1966), and W. E. Brown in "International Symposium on Structural Properties of Hydroxyapatite and Related Compounds, Gaithersburg, Md., Sept 12–14, 1968," Gordon and Breach, New York, N. Y., in press, for summary of causes of nonstoichiometry.

(2) O. R. Trautz, *Ann. N. Y. Acad. Sci.*, 60, 696 (1955).

(3) H. C. W. Skinner, *Amer. J. Sci.*, in press.

(4) B. O. Fowler, *Inorg. Chem.*, 13, 194 (1974).

(5) In reactions 2 and 3, $10MO{\cdot}3P_2O_5$ represents the gross chemical composition of the intermediate solid phase.